AIMS Mathematics, 11(3): 8417–8427.
DOI: 10.3934/math.2026346
Received: 04 January 2026
Revised: 07 March 2026
Accepted: 16 March 2026
Published: 30 March 2026

https://www.aimspress.com/journal/Math

Research article

Bifurcation analysis and novel traveling wave solutions for the (4+1)-dimensional Fokas equation with variable coefficients

Rehab M. El-Shiekh[1,*] **and Mahmoud Gaballah**[2,3]

[1] Department of Business Administration, College of Business Administration in Majmaah, Majmaah University, Al-Majmaah City, 11952, Saudi Arabia
[2] Department of Physics, College of Science at Al-Zulfi, Majmaah University, Al-Majmaah City, 11952, Saudi Arabia
[3] Geomagnetic and Geoelectric Department, National Research Institute of Astronomy and Geophysics (NRIAG), 11421 Helwan, Cairo, Egypt

* **Correspondence:** Email: r.abdelhaim@mu.edu.sa.

Abstract: In this paper, the variable-coefficient (4+1)-dimensional Fokas (4D-vc Fokas) equation, which describes the evolution of water waves with surface tension in ocean dynamics, is studied using bifurcation analysis. The dynamic system and phase portrait are presented and discussed graphically. Then, the whole discrimination system of the 4D-vc Fokas equation was discussed to classify the possible analytic traveling wave solutions; as a result, novel solitary waves and periodic waves were yielded by setting specific relationships between the coefficients. The soliton wave's motion was affected by the choices of the variable coefficients and took a parabolic and periodic shape; it also became a bright or dark soliton.

Keywords: (4+1)-dimensional variable-coefficient Fokas equation; bifurcation analysis; discrimination system; traveling waves
Mathematics Subject Classification: 35-XX, 35C08

1. Introduction

The study of higher-dimension nonlinear partial differential equations (NPDEs) became very important in recent days because these types of NPDEs describe complex phenomena in different engineering and physics aspects. In 2006, Fokas [1] introduced one of those higher dimensional NPDEs, the (4+1)-dimensional Fokas equation, which was a higher extension of two related equations, the Davey-Stewartson (DS) equation and the Kadomtsev-Petviashvili (KP) equation. According to that, the Fokas equation could have many different applications in fluid mechanics,

hydrodynamics, and ocean engineering, where it can be used to describe complex wave propagation; it can also be applied in the field of optics and the study of nonlinear pulse transmission that can take place in mono-mode optical fibers [2–4]. Therefore, the Fokas equation serves as a powerful mathematical tool to model and understand the behavior of high-dimensional nonlinear waves in diverse physical systems across physics and various branches of engineering.

$$4v_{xt} - 6v_{zw} - v_{xxxy} + v_{xyyy} + 12\left(v_x v_y + v v_{xy}\right) = 0, \tag{1.1}$$

where v represents the wave function, t is the time and x, y, z, w are the space variables. The previous constant version of the Fokas equation has been solved using different techniques like the modified tanh-coth method, the Exp-function method, the extended Jacobi elliptic function method, Lie group analysis, etc. [5–7].

As the variable coefficients of NPDEs describe the phenomena in realistic physical situations than the constant coefficients of NPDEs and are considered a challenge to solve analytically [8–10]. Therefore, in this paper, we are going to discuss the (4+1)-dimensional variable-coefficient Fokas (vc-Fokas) equation given by [11–13].

$$\alpha(t)\, v_{xt} - \beta(t)\left(v_{xxxy} + v_{xyyy}\right) + \delta(t)\left(v_x v_y + v v_{xy}\right) + a(t)\, v_{zw} = 0, \tag{1.2}$$

where $\alpha(t)$ refers to the time-dependent velocity or amplitude scaling of the wave, $\beta(t)$ models the effect of slowly varying bathymetry (water depth) in ocean engineering or the inhomogeneity of the medium (e.g., density or refractive index) in optics, $\delta(t)$ is the nonlinear effect coefficient, and $a(t)$ represents a time-varying constraint in higher dimensions [11, 12]. Equation (1.2) has been solved recently by Hirota's bilinear method and Bäcklund transformation, where one, two, and three soliton solutions were obtained, and they used the test method also to obtain lump and breather solutions [11, 12]. Equation (1.2) was reduced to a nonlinear ordinary differential equation in [13], and Jacobi elliptic wave solutions were obtained.

Given the importance of the higher-dimensional variable-coefficient nonlinear evolution equations (NLEEs) and the sparse studies done on the (4+1)-dimensional variable-coefficient Fokas (4D-vc Fokas) equation, we are going to study this equation using bifurcation analysis and a discrimination system, to find phase portraits and novel traveling wave solutions of the 4D vc-Fokas equation under the necessary conditions between the variable coefficients. Moreover, a key contribution of the study is demonstrating how the variable coefficients—which depend on time—directly manipulate the wave's physical behavior, causing solitons to adopt parabolic or periodic shapes and transition between bright and dark states. By establishing specific constraints between these coefficients, the research provides a deeper qualitative and quantitative understanding of wave trajectories in realistic, complex physical scenarios

2. Dynamic system and phase portraits

A phase portrait is a graphical representation of the trajectories of a dynamic system in its phase space. It is a powerful tool for visualizing the qualitative behavior of a system without having to solve the equations explicitly. Each curve or arrow in a phase portrait represents a possible path or trajectory that the system could take over time, starting from a given initial condition. A collection of these trajectories gives a complete picture of the system's dynamics [14–16].

To able to reduce the 4D vc-Fokas equation to a nonlinear ordinary differential equation, we have used the traveling wave transformation

$$v(x,y,z,w,t) = f(\eta), \eta = c_1x + c_2y + c_3z + c_4w - \varphi(t), \tag{2.1}$$

where c_j, $j = 1, ..., 4$ are nonzero constants and $\varphi(t) \in C^1$ is an arbitrary function of t. By substitution from Eq (2.1) in (1.2), the 4D vc-Fokas equation can be rewritten as:

$$\beta(t)\left(c_1^3c_2 + c_1c_2^3\right)f^{(4)} - \left(c_3c_4a(t) - c_1\alpha(t)\frac{d\varphi(t)}{dt}\right)f'' - c_1c_2\delta(t)(f'f)' = 0. \tag{2.2}$$

By dividing the Eq (2.2) terms by the linear coefficient and integrating it twice with respect to η, we get:

$$f'' = \frac{\delta(t)}{2\beta(t)\left(c_1^2 + c_2^2\right)}f^2 - \frac{\left(c_1\alpha(t)\frac{d\varphi(t)}{dt} - c_3c_4a(t)\right)}{\beta(t)c_1c_2\left(c_1^2 + c_2^2\right)}f + C_1\eta + C_2, \tag{2.3}$$

where C_1 and C_2 are integration constants. To make Eq (2.3) integrable and to be able to find the Hamiltonian system and bifurcation analysis we assume that C_1 is finished. Moreover, in order to obtain localized traveling wave solutions satisfying vanishing boundary conditions at infinity, C_2 also will be finished. Now, assume that the coefficients of f and f^2 are the constants A_1 and A_2 respectively:

$$A_1 = \frac{\delta(t)}{2\beta(t)\left(c_1^2 + c_2^2\right)} \text{ and } A_2 = \frac{\left(c_1\alpha(t)\frac{d\varphi(t)}{dt} - c_3c_4a(t)\right)}{\beta(t)c_1c_2\left(c_1^2 + c_2^2\right)}. \tag{2.4}$$

From Eq (2.4), constraints arise between the variable coefficients as follows:

$$\varphi(t) = \int\left(\frac{c_3c_4a(t)}{c_1\alpha(t)} + \frac{\beta(t)\left(c_1^2c_2 + c_2^3\right)}{\alpha(t)}A_2\right)dt, \delta(t) = 2A_1\beta(t)\left(c_1^2 + c_2^2\right). \tag{2.5}$$

Now, Eq (2.3) can be rewritten as

$$f'' = A_1f^2 - A_2f. \tag{2.6}$$

The reduced Eq (2.6) is obtained directly from Eq (2.3) by defining A_1 and A_2 as in Eq (2.4). The sign in front of the linear term is preserved consistently so that the equation admits the dynamic system

$$\begin{aligned} f'(\eta) &= g(\eta), \\ g'(\eta) &= A_1f^2 - A_2f, \end{aligned} \tag{2.7}$$

with the Hamiltonian structure

$$H(f,g) = \frac{1}{2}g^2 + V(f) = h, \tag{2.8}$$

where h is a constant. Hamiltonian (2.8) describes the one-dimensional motion of a particle under the influence of a one-parameter potential V, whose specific form is

$$V(f) = -\frac{A_1}{3}f^3 + \frac{A_2}{2}f^2. \tag{2.9}$$

For linearization and stability analysis, the Jacobian matrix of System (2.7) is given by

$$J(f,g) = \begin{pmatrix} 0 & 1 \\ 2A_1 f - A_2 & 0 \end{pmatrix}. \tag{2.10}$$

System (2.7) has two equilibrium points, $P_1 = (0,0)$ and $P_2 = (\frac{A_2}{A_1}, 0)$, at $P_1 = (0,0)$ from the Jacobian matrix, the characteristic equation is $\lambda^2 + A_2 = 0$ so the eigenvalues are $\lambda = \pm i\sqrt{A_2}$. Similarly, at $P_2 = (\frac{A_2}{A_1}, 0)$, the characteristic equation is $\lambda^2 - A_2 = 0$ and the eigenvalues are $\lambda = \pm\sqrt{A_2}$. Therefore, we have two different cases.

Case 2.1. If $A_2 > 0$, then the eigenvalues at P_1 are purely imaginary and P_1 is a center point, but the eigenvalues at P_2 are real and P_2 is a saddle point (Figure 1(a)). In this figure, we can see that the trajectories are closed orbits surrounding the center point P_1 and it represents periodic traveling wave's solutions, where the wave amplitude oscillates around the equilibrium value of $f = 0$. P_1, as a center point, indicates orbital stability; therefore, the periodic wave solutions are stable. The single trajectory that approaches and leaves the saddle point P_2 is homoclinic orbit corresponds to a solitary wave solution, so it is marginally stable or conditionally unstable.

Case 2.2. If $A_2 < 0$, then the eigenvalues at P_2 are purely imaginary and P_2 is a center point, but the eigenvalues at P_1 are real and P_1 is a saddle point according to Figure 1(b). In this case, the roles of the equilibrium points are reversed. The loops surrounding the center point are periodic solutions, where the wave's amplitude oscillates around the equilibrium value of $f = P_2$. The periodic wave solutions oscillating around P_2 are stable. The separatrix approaches and leaves the saddle point P_1 corresponding to the solitary wave solution which is marginally stable or conditionally unstable.

Figure 1 shows two different cases of the phase portrait, plotted by considering $A_2 = \pm 1$, and we have a fixed $A_1 = 1$, where the solid red circles indicate the equilibrium points. Moreover, the potential function V is plotted according to $A_2 = \pm 1$ in Figure 1(c),(d).

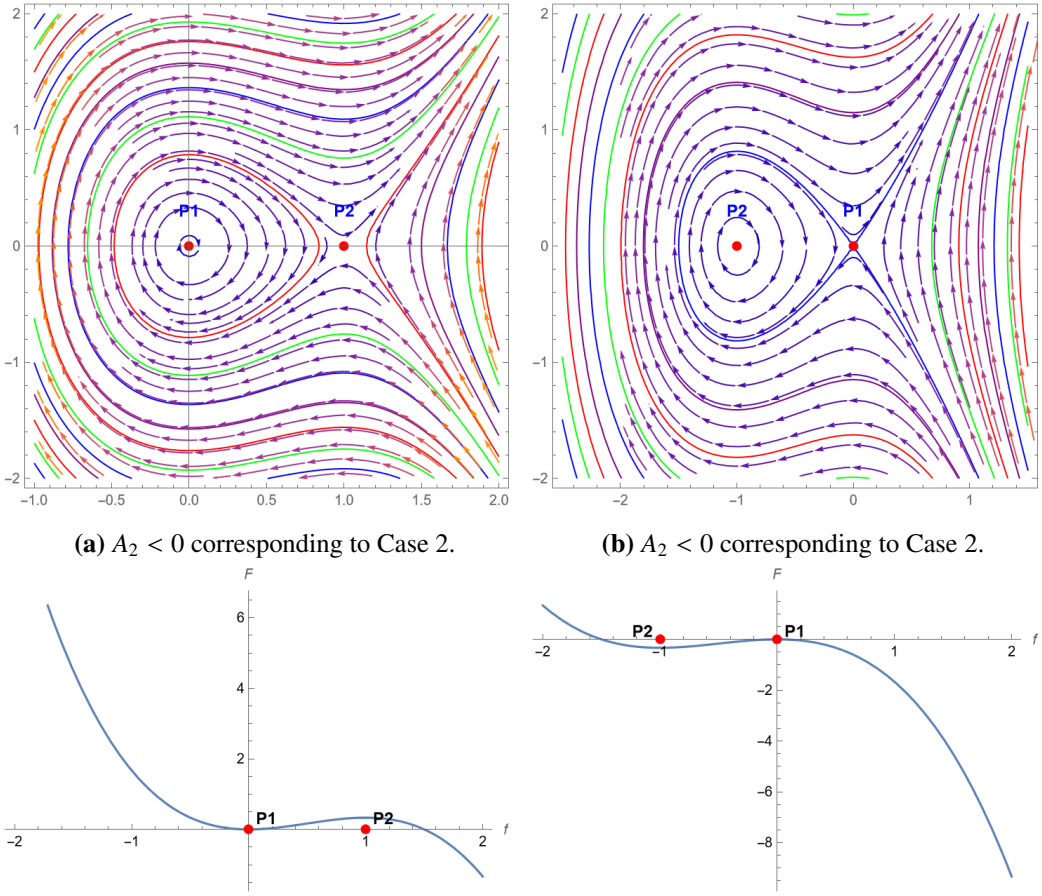

(a) $A_2 < 0$ corresponding to Case 2.

(b) $A_2 < 0$ corresponding to Case 2.

(c) The function V when $A_2 > 0$.

(d) The function V when $A_2 < 0$.

Figure 1. The two different cases of the phase portrait, where plotted by considering $A_2 = \pm 1$ in Figure 1(a),(b), and we have a fixed $A_1 = 1$, where the solid red circles indicate the equilibrium points. Moreover, the potential function V is plotted according to $A_2 = \pm 1$ in Figure 1(c),(d).

3. Discrimination system of the 4D vc-Fokas equation

A complete discrimination system is a set of algebraic conditions used to classify the exact traveling wave solutions. This system is derived from the properties of a related polynomial, which itself is obtained by transforming the PDE into an ordinary differential equation. The term "discrimination" here relates to the mathematical concept of a discriminant, which is function of the coefficients of a polynomial equation that provides information about the nature of its roots [17–19].

To obtain a new traveling wave solution for the 4D vc-Fokas equation depending on the phase portrait and the whole discrimination of the Hamiltonian system given by Eq (2.8), we can rewrite it as

$$f'^2 = \frac{2}{3}A_1 f^3 - A_2 f^2 + h. \tag{3.1}$$

From previous studies [17] about the complete discrimination system for the third-degree polynomial,

we put

$$u = (\frac{2}{3}A_1)^{\frac{1}{3}} f, b_2 = -A_2(\frac{2}{3}A_1)^{\frac{-2}{3}}, b_0 = (\frac{2}{3}A_1)^{\frac{1}{3}} h \tag{3.2}$$

Then Eq (3.1) can be rewritten as:

$$\pm (\frac{2}{3}A_1)^{\frac{1}{3}}(\eta - \eta_0) = \int \frac{df}{\sqrt{u^3 + b_2u^2 + b_0}}, \tag{3.3}$$

where η_0 is the integration constant. The complete discrimination system for the third-degree polynomial $U(u) = u^3 + b_2u^2 + b_0$ is given by $\triangle = -27\left(\frac{2b_2^3}{27} + b_0\right)^2 + \frac{4}{27}b_2^6$ and $D = -\frac{b_2^2}{3}$, the following three cases are raised for solutions.

Case 3.1. Where $\triangle = 0$ and $h = 0$, the polynomial $U(u)$ has two real roots, one double (its value is zero) and one simple; its value is $-b_2 = A_2(\frac{2}{3}A_1)^{\frac{-2}{3}}$.Therefore, the phase portrait contains a homoclinic orbit corresponding to the following solitary wave solutions of the vc-Fokas equation where $A_2 < 0$, where the red color trajectory in Figure 1(b) cuts the f-axis into two points, one of them being the saddle point P_1,

$$v_1 = \frac{3A_2}{2A_1}\ sech^2\left(\frac{\sqrt{-A_2}}{2}(\eta - \eta_0)\right), \quad A_2 < 0, \tag{3.4}$$

$$v_2 = \frac{3A_2}{2A_1}\ csch^2\left(\frac{\sqrt{-A_2}}{2}(\eta - \eta_0)\right), \quad A_2 < 0, \tag{3.5}$$

and when $A_2 > 0$, closed orbits surround the center point P_1, and periodic wave solutions are given for the vc-Fokas equation represented by the blue line in Figure 1(a)

$$v_3 = \frac{3A_2}{2A_1}\ \sec^2\left(\frac{\sqrt{A_2}}{2}(\eta - \eta_0)\right), \qquad A_2 > 0. \tag{3.6}$$

$$v_4 = \frac{3A_2}{2A_1}\ \csc^2\left(\frac{\sqrt{A_2}}{2}(\eta - \eta_0)\right), \qquad A_2 > 0. \tag{3.7}$$

Case 3.2. If $\triangle > 0$, then there are three distinct roots and the polynomial $U(u) = (u-u_1)(u-u_2)(u-u_3)$. Assume that $u_1 < u_2 < u_3$ and $u_1 < u < u_2$, so we have the following new periodic wave solution for the 4D vc-Fokas equation:

$$v_5 = (\frac{2}{3}A_1)^{\frac{-1}{3}}\left(u_1 + (u_2 - u_1)\ sn^2\left(\frac{\sqrt{u_3 - u_1}}{2}(\frac{2}{3}A_1)^{\frac{1}{3}}(\eta - \eta_0), m\right)\right), \tag{3.8}$$

where $m = \frac{u_2-u_1}{u_3-u_1}$.

Case 3.3. If $\triangle < 0$, then the polynomial $U(u) = (u - u_1)(u^2 + pu + q)$, $p^2 - 4q < 0$. Assume that $u_1 < u_2 < u_3$ and $u_1 < u < u_2$. According to that, we have the following novel periodic wave solution for the 4D vc-Fokas equation:

$$v_6 = (\frac{2}{3}A_1)^{\frac{-1}{3}}\left(u_1 - \sqrt{u_1^2 + pu_1 + q} + \frac{2\sqrt{u_1^2 + pu_1 + q}}{1 + cn\left(\left(u_1^2 + pu_1 + q\right)^{\frac{1}{4}}(\frac{2}{3}A_1)^{\frac{1}{3}}(\eta - \eta_0), m\right)}\right), \tag{3.9}$$

where $m^2 = \frac{1}{2}\left(1 - \frac{u_1 + \frac{p}{2}}{\sqrt{u_1^2+pu_1+q}}\right)$.

4. Physical applications and dynamic behavior

Solitary waves, or solitons, are remarkable because they maintain their shape and speed over long distances [22–24]. They emerge from a perfect balance between two opposing forces: The tendency of a wave to steepen due to nonlinear effects and its tendency to spread out due to dispersive effects [25, 26]. This unique equilibrium allows them to exist as a single, self-reinforcing wave packet with a localized peak that quickly diminishes on either side [27–29]. In this section, a visualization of the soliton solution v_1 will be given according to three different values of the variable coefficients to show how those coefficients affect the soliton's motion and the wave's behavior. We have fixed the parameters as: $y = z = w = 0, c_1 = c_2 = c_3 = c_4 = 1, A_2 = -1$.

In Figures 2 and 3 we have plotted v_1 in both x and t dimension and the same can be done in other dimensions with the time t replacing x by y or z or w. We have found that the soliton's direction affected with the sign of A_1=$\mp$1, and it becomes bright or dark in Figures 2 and 3 respectively. Additionally, we have the choice $a(t) = \beta(t) = \alpha(t) = t$ in Figures 2(a) and 3(a) and we obtained bright and dark soliton shapes. In Figures 2(b) and 3(b) we assumed that $a(t) = \beta(t) = t, \alpha(t) = 1$, and in this case, the parabolic effect is higher. Finally in Figures 2(c) and 3(c) we have taken the variables as a sine function $a(t) = \beta(t) = \sin(t), \alpha(t) = 1$ and a periodic effect appears. Therefore, the sign of A_1 affects the direction of the soliton (bright or dark) and the choices of the variable function affect the shape of the soliton.

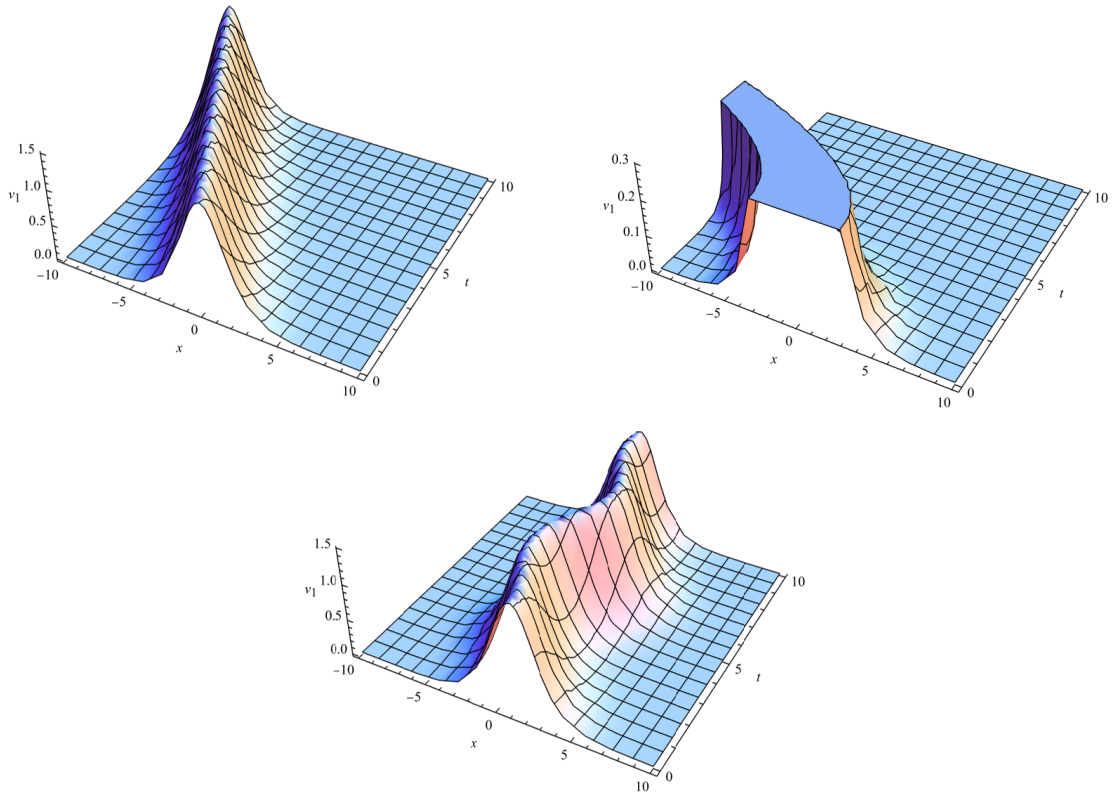

Figure 2. The bright soliton solution, where v_1 changes in its shape from one figure to another according the change in the variable coefficient as $a(t) = \beta(t) = \alpha(t) = t$ in (a), $a(t) = \beta(t) = t, \alpha(t) = 1$ in (b), and $a(t) = \beta(t) = \sin(t), \alpha(t) = 1$ in (c), where $A_1 = -1$.

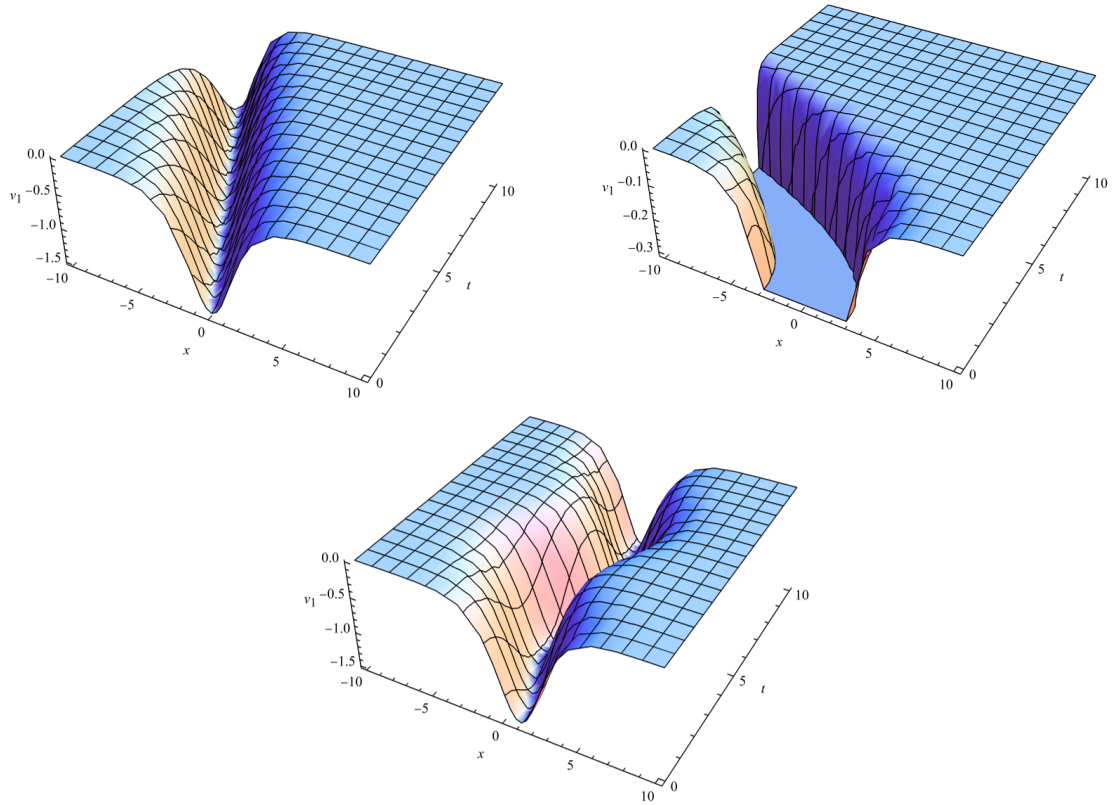

Figure 3. The dark soliton solution, where v_1 changes in its shape from one figure to another according the change in the variable coefficient as $a(t) = \beta(t) = \alpha(t) = t$ in (a), $a(t) = \beta(t) = t, \alpha(t) = 1$ in (b), and $a(t) = \beta(t) = \sin(t), \alpha(t) = 1$ in (c), where $A_1 = 1$.

5. Conclusions

According to the study of the 4D-vc Fokas equation using bifurcation analysis, we have found two equilibrium points, and the trajectories of the dynamic system in its phase space were presented in relation to two different cases with graphical representation. The bifurcation analysis reveals that the qualitative dynamics of the reduced system is governed by the parameters A_1 and A_2, which depend on the variable coefficients of the original equation. Consequently, the time-dependent physical parameters determine whether the system generates periodic waves or localized solitons and control their polarity (bright or dark). This provides a dynamic interpretation of the wave behavior described by the variable-coefficient (4+1)-dimensional Fokas equation. The complete discrimination system of the reduced nonlinear ordinary differential equation of the 4D-vc Fokas equation is presented, and all possible travelling wave solutions were constructed. Therefore, novel soliton and periodic wave solutions are given. Moreover, the soliton wave solution is plotted for different values of the variable coefficients, and it was found that it takes a parabolic shape and a periodic shape depending on the variable choices. One of the constants given was where we reduced the 4D-vc Fokas equation A_1; if its sign is negative, the soliton wave became bright, but if the sign is positive, it became dark.

Author contributions

Rehab M. Elshiekh wrote and applied different methodologies, and Mahmoud Gaballah made physical applications and the figures. All authors have read and agreed to publish the manuscript.

Use of Generative-AI tools declaration

The authors declare that they have not used artificial intelligence (AI) tools in the creation of this article.

Acknowledgments

The authors would like to thank the Deanship of Graduate Studies and Scientific Research, Majmaah University, Kingdom of Saudi Arabia, for funding this work under project number: R-2026-111.

Conflict of interest

There is no conflict of interest.

References

1. A. S. Fokas, Integrable nonlinear evolution partial differential equations in 4+2 and 3+1 dimensions, *Phys. Rev. Lett.*, **96** (2006), 190201. https://doi.org/10.1103/PhysRevLett.96.190201
2. G. Akram, M. Sadaf, M. A. U. Khan, Dynamics investigation of the (4+1)-dimensional Fokas equation using two effective techniques, *Results Phys.*, **42** (2022), 105994. https://doi.org/10.1016/J.RINP.2022.105994
3. J. Lee, R. Sakthivel, L. Wazzan, Exact traveling wave solutions of a higher-dimensional nonlinear evoultion equation, *Mod. Phys. Lett. B*, **24** (2011), 1011–1021. https://doi.org/10.1142/S0217984910023062
4. S. Kumar, M. Niwas, M. S. Osman, M. A. Abdou, Abundant different types of exact soliton solution to the (4+1)-dimensional Fokas and (2+1)-dimensional breaking soliton equations, *Commun. Theor. Phys.*, **73** (2021), 105007. https://doi.org/10.1088/1572-9494/AC11EE
5. R. M. El-Shiekh, M. Gaballah, Similarity reduction, Bäcklund transformation and solitary waves for a generalized shallow water wave equation with the variable coefficients, *Ain Shams Eng. J.*, **16** (2025), 103618. https://doi.org/10.1016/J.ASEJ.2025.103618
6. R. M. El-Shiekh, M. Gaballah, Novel optical waves for the perturbed nonlinear Chen-Lee-Liu equation with variable coefficients using two different similarity techniques, *Alex. Eng. J.*, **86** (2024), 548–555. https://doi.org/10.1016/J.AEJ.2023.12.003
7. M. Gaballah, R. M. El-Shiekh, Bäcklund transformation, similarity reduction and new solutions for the (2+1)-dimensional graphene sheets thermophoretic motion equation with variable heat transmission, *Alex. Eng. J.*, **95** (2024), 24–29. https://doi.org/10.1016/J.AEJ.2024.03.046

8. R. M. El-Shiekh, M. Gaballah, Bright and dark optical chirp waves for Kundu–Eckhaus equation using Lie group analysis, *Z. Naturforsch. A*, **80** (2025), 1–7. https://doi.org/10.1515/zna-2024-0154
9. M. Gaballah, R. M. El-Shiekh, Novel nonlinear quantum dust acoustic waves for modified variable coefficients Zakharove–Kusnetsov equation in dusty plasma, *Math. Method. Appl. Sci.*, **47** (2024), 11530–11538. https://doi.org/10.1002/MMA.10141
10. M. Gaballah, R. M. El-Shiekh, Symmetry transformations and novel solutions for the graphene thermophoretic motion equation with variable heat transmission using Lie group analysis, *EPL*, **145** (2024), 12002. https://doi.org/10.1209/0295-5075/AD19E5
11. Y. Wang, X. Lü, Exact solutions and Bäcklund transformation for a generalized (3+1)-dimensional variable-coefficient Fokas-typed equation, *Commun. Nonlinear Sci.*, **143** (2025), 108567. https://doi.org/10.1016/J.CNSNS.2024.108567
12. H. Yang, B. He, Bilinear Bäcklund transformations, lump solutions and interaction solutions for (4+1)-dimensional variable-coefficient Fokas equation, *Z. Angew. Math. Phys.*, **74** (2023), 155. https://doi.org/10.1007/s00033-023-02052-3
13. R. M. El-Shiekh, M. Gaballah, Similarity reduction and novel Jacobi wave solutions for the variable (4+1)-dimensional Fokas equation, *AIMS Math.*, **10** (2025), 23869–23879. https://doi.org/10.3934/math.20251061
14. H. W. A. Riaz, A. Farooq, Exploring soliton solutions of coupled dispersionless equations with new insights into bifurcation, chaos, and sensitivity through advanced analytical techniques, *Opt. Quant. Electron.*, **56** (2024), 1784. https://doi.org/10.1007/s11082-024-07615-w
15. M. K. Alaoui, M. M. Roshid, M. Uddin, W. X. Ma, H. O. Roshid, M. J. H. Munshi, Modulation instability, bifurcation analysis, and ion-acoustic wave solutions of generalized perturbed KdV equation with M-fractional derivative, *Sci. Rep.*, **15** (2025), 11923. https://doi.org/10.1038/S41598-024-84941-9
16. A. R. Ali, H. O. Roshid, S. Islam, A. Khatun, Analyzing bifurcation, stability, and wave solutions in nonlinear telecommunications models using transmission lines, Hamiltonian and Jacobian techniques, *Sci. Rep.*, **14** (2024), 15282. https://doi.org/10.1038/s41598-024-64788-w
17. W. M. Hasan, W. B. Rabie, A. M. Ahmed, H. M. Rezk, H. M. Ahmed, Construction of new travelling wave solutions and bifurcation analysis for the (2+1)-dimensional extended KP-BO equation utilizing the improved modified extended tanh-function method, *Int. J. Comput. Math.*, **102** (2025), 2214–2227. https://doi.org/10.1080/00207160.2025.2541068
18. Z. A. Alhussain, Exploring multi-soliton patterns, bifurcation analysis, and chaos in (2+1) dimensions: A study on nonlinear dynamics, *Ain Shams Eng. J.*, **15** (2024), 102917. https://doi.org/10.1016/J.ASEJ.2024.102917
19. C. S. Liu, Applications of complete discrimination system for polynomial for classifications of traveling wave solutions to nonlinear differential equations, *Comput. Phys. Commun.*, **181** (2010), 317–324. https://doi.org/10.1016/J.CPC.2009.10.006
20. S. Zhao, Multiple solutions and dynamical behavior of the periodically excited beta-fractional generalized KdV-ZK system, *Phys. Scripta*, **100** (2025), 045244. https://doi.org/10.1088/1402-4896/ADC20C

21. S. Zhao, Z. Li, The analysis of traveling wave solutions and dynamical behavior for the stochastic coupled Maccari's system via Brownian motion, *Ain Shams Eng. J.*, **15** (2024), 103037. https://doi.org/10.1016/J.ASEJ.2024.103037

22. C. H. Gu, *Soliton theory and its applications*, Berlin, Heidelberg: Springer, 1995. https://doi.org/10.1007/978-3-662-03102-5

23. W. P. Zhong, Z. Yang, M. Belić, Dark beam excitations in the defocusing (2+1)-dimensional Zakharov system, *Phys. Lett. A*, **480** (2023), 128969. https://doi.org/10.1016/j.physleta.2023.128969

24. D. S. Mou, Z. Z. Si, W. X. Qiu, C. Q. Dai, Optical soliton formation and dynamic characteristics in photonic Moiré lattices, *Opt. Laser Technol.*, **181** (2025), 111774. https://doi.org/10.1016/j.optlastec.2024.111774

25. D. Wang, Z. Liu, H. Zhao, H. Qin, G. Bai, C. Chen, et al., Launching by cavitation, *Science*, **389** (2025), 935–939. https://doi.org/10.1126/science.adu8943

26. Z. Z. Si, D. L. Wang, B. W. Zhu, Z. T. Ju, X. P. Wang, W. Liu, et al., Deep learning for dynamic modeling and coded information storage of vector-soliton pulsations in mode-locked fiber lasers, *Laser Photonics Rev.*, **18** (2024), 2400097. https://doi.org/10.1002/lpor.202400097

27. Z. Yang, W. P. Zhong, M. Belić, Dark localized waves in shallow waters: Analysis within an extended Boussinesq system, *Chinese Phys. Lett.*, **41** (2024), 044201. https://doi.org/10.1088/0256-307X/41/4/044201

28. J. Yang, Y. Zhu, W. Qin, S. Wang, J. Li, 3D bright-bright Peregrine triple-one structures in a nonautonomous partially nonlocal vector nonlinear Schrodinger model under a harmonic potential, *Nonlinear Dynam.*, **111** (2023), 13287–13296. https://doi.org/10.1007/s11071-023-08526-3

29. Z. T. Ju, Z. Z. Si, X. Yan, C. Q. Dai, Solitons and their biperiodic pulsation in ultrafast fiber lasers based on CB/GO, *Chinese Phys. Lett.*, **41** (2024), 084203. https://doi.org/10.1088/0256-307X/41/8/084203

AIMS Press

© 2026 the Author(s), licensee AIMS Press. This is an open access article distributed under the terms of the Creative Commons Attribution License (https://creativecommons.org/licenses/by/4.0)